

**Konrad Lewacki\*, Marta Smektała\*\*,  
Magdalena Baborska-Narożny\*\*\***

***Generalization of GIS data as a tool supporting  
the understanding of the urban heat island effect.  
Case study of the city of Wrocław based on design experience***

***Abstract***

The article presents how various urban factors influence the urban heat island (UHI) effect and explores the correlations between these factors. The authors attempt to verify the potential of using data in Geographic Information System (GIS) analyses to study the urban heat island effect, and in further research to analyze the potential for nighttime cooling in the city, using Wrocław as a case study. The study utilized Landsat 8 satellite imagery and spatial data on greenery and built-up areas to analyze their impact on radiative temperature. The proposed method simplifies and calibrates data, enabling comparison of different areas. It also allows for the analysis of relationships between the values of various factors within a single grid cell or study area. This approach helps identify areas across the entire city with similar factor combinations and compare their temperature distributions. GIS analyses enable examination of neighboring areas and identification of other factors influencing variations in radiative temperature.

The research presents how individual factors affect ambient temperature. Building density and height significantly increase radiative temperature, whereas the presence of water and greenery, especially in large amounts, has a cooling effect. To assess temperature distribution differences in urban spaces, four locations in Wrocław were compared based on building intensity and greenery levels: Przedmieście Oławskie, Przedmieście Świdnickie, Plac Grunwaldzki, and Olimpia Port. Results indicate that despite the presence of a river, Przedmieście Oławskie has the highest radiative temperature due to dense building and low greenery. In contrast, Olimpia Port, with the lowest building density and highest greenery, is the coolest area.

The aim of the research is to indicate the representative areas in urban tissue, where further research measuring the local air temperature can be implemented. Future stages of the project plan to include additional factors such as air flow, impermeable surface area, and building materials to further investigate the impact of urban planning on ambient temperature.

**Key words:** GIS analysis, urban heat island, Landsat analysis, radiation temperature, natural cooling potential

***Introduction***

The limited extent of urban green spaces and the high degree of urbanization significantly contribute to the intensification of the urban heat island (UHI) effect – a climatic phenomenon characterized by elevated temperatures with-

in urban areas compared to their rural surroundings (EPA 2025). The magnitude of the UHI effect is further exacerbated by the expansion of urbanized zones, commonly referred to as urban sprawl (Gawuś et al. 2020; Błażejczyk, Błażejczyk 2023). The UHI phenomenon is typically analyzed through three distinct dimensions: subsurface, surface, and atmospheric, each assessed using different methodological approaches (Huang et al. 2020). Current research explores the variability of temperature within these dimensions, as well as the interrelations among them, across diverse climatic and urban configurations (Wonorahardjo et al. 2022; Deilami, Kamruzzaman and Liu 2018). The present study contributes to this research agenda by examining the potential of

\* ORCID: 0009-0007-0886-2755. Faculty of Architecture, Wrocław University of Science and Technology, Poland.

\*\* ORCID: 0000-0001-8533-8550. Faculty of Architecture, Wrocław University of Science and Technology, Poland, e-mail: marta.smektala@pwr.edu.pl.

\*\*\* ORCID: 0000-0001-6860-5186. Faculty of Architecture, Wrocław University of Science and Technology, Poland.

spatial surface temperature variation as a proxy for analyzing air temperature differentials in the vicinity of buildings.

Studies conducted in Poland's regional capital cities between 1971 and 2020 have indicated a continuous increase in the number of tropical nights – defined as nights during which air temperature does not drop below 20°C. This phenomenon is particularly pronounced in cities located in western Poland (Mąkosza et al. 2024). It is important to note, however, that meteorological data are typically collected from stations intentionally situated away from urbanized areas. Consequently, air temperatures in city centers – where building materials accumulate heat more intensely – may differ significantly from those recorded at monitoring stations located in suburban areas (Eliasson, Svensson 2003; Baborska-Narożny, Kostka and Smektała 2024). As a result, the actual number of tropical nights within densely built-up urban environments may be substantially higher. Tropical nights are known to impair sleep quality and negatively impact cardiovascular and respiratory function (Buguet et al. 2023). Daytime heat, compounded by the reduced potential for nighttime cooling in built-up areas, intensifies thermal stress, adversely affecting human health and contributing to increased mortality rates (Peng et al. 2022; Błażejczyk et al. 2022; Runhaar et al. 2012). Heatwaves may also exacerbate the detrimental effects of air pollution and increase plants' allergen production (Pałczyński et al. 2018). It is estimated that during the summer of 2022 alone, excessive heat caused 61,672 deaths across Europe (WHO 2024). Globally, the number of people exposed to extreme temperatures is increasing exponentially as a result of climate change. Heat-related mortality among individuals aged 65 and older rose by approximately 85% between 2017–2021 compared to 2000–2004 (WHO 2024). The adverse impacts of thermal stress are especially severe for the elderly, persons with disabilities, and socially marginalized groups. Residents from economically disadvantaged neighborhoods often live farther from green spaces and typically inhabit poorly insulated homes lacking air conditioning (Jessel, Sawyer and Hernández 2019; Lundgren-Kownacki et al. 2018). While the use of air conditioning can mitigate heat stress, it simultaneously increases energy consumption – particularly from non-renewable sources – thereby contributing to further climate warming. Moreover, it can elevate local outdoor temperatures, especially in densely built urban canyon environments. Therefore, it is essential to explore alternative urban and architectural adaptation strategies. These include deliberate design of urban geometry and building density, integration of green infrastructure and water bodies, as well as building-level measures such as thermal insulation and solar gain control. Given the complexity of interventions required to reshape urban systems, the implementation of such changes may span several decades – amid ongoing climate warming (Viguié et al. 2020).

Wrocław, along with Warsaw, Rzeszów, Łódź, and Kraków, is one of the 100 European cities participating in the so-called Mission for Climate-Neutral and Smart Cities (Serwis Rzeczypospolitej Polskiej 2022). The authorities of these cities have committed to developing agreements that include a comprehensive plan for climate neutrality

across all sectors, such as energy, construction, waste management, and transport, along with associated investment plans. The study presented in this article is part of the project “Summer in the City (Without Air Conditioning) – A Map of Night Cooling Potential and the Wrocław Urban Heat Island.” The goal of the project is to fit the scope of challenges set by cities aiming climate neutrality by examining whether appropriate urban planning, architectural, and ventilation strategies can reduce the reliance on air conditioning in Wrocław and take advantage of building thermal mass night cooling potential to maintain indoor thermal comfort (de Toldi, Craig, and Sushama 2022).

Results from previous studies indicate that despite a warming climate, buildings located in Central and Northern Europe will be able to benefit from night cooling potential at least for the coming decades (Artmann et al. 2008). However, a publication concerning the UHI in Warsaw indicated that the number of hot days requiring the use of air conditioning may increase by more than 120% by the end of the 21<sup>st</sup> century – from 32–34 to 76 days annually (Błażejczyk et al. 2014). At present, merely 10% of households in Europe are equipped with air conditioning, whereas in the United States this figure reaches as high as 90% (IEA 2023). To prevent increasingly frequent and intense heatwaves from causing a surge in air conditioning use in Central and Northern European cities, it is essential to explore the potential for reducing residential overheating through passive solutions associated with appropriate architectural and urban design. The effectiveness of passive solutions, such as night cooling via natural ventilation, depends, among other factors, on the outdoor air temperature. Therefore it is closely linked to the local intensity of the urban heat island (UHI). For this reason, understanding the mechanisms responsible for urban overheating, which influence the UHI effect, is crucial for the effective implementation of passive cooling strategies.

In the article *Klimat Wrocławia* [The Climate of Wrocław], an instance of a particularly intense surface urban heat island (SUHI) effect in Wrocław was described, occurring during the night of May 22–23, 2001. At that time, under cloudless skies and low wind conditions, satellite imagery capturing surface radiative temperature revealed a difference of over 8°C between the city center and its outskirts (Dubicki, Dubicka and Szymanowski 2002). This observation was made more than two decades ago, and since then the city has undergone significant development, likely expanding the area affected by elevated temperatures. In 2023, the Institute of Meteorology and Water Management (IMGW) named Wrocław the hottest city in Poland, with the highest annual mean temperature of 11.3°C (IMGW 2024). These and other factors motivated the authors to investigate the topic addressed in this study. The aim is to explore the following research questions:

1. How can the relationship between the distribution of surface radiative temperature and urban indicators describing built-up areas and greenery be visualized within a given urban unit?

2. How can the proposed GIS-based analytical method be applied to examine the influence of these factors on the urban heat island effect and the potential for nighttime cooling?

## **Urban heat island and GIS analyses – state of research**

Despite increasing interest and growing knowledge about the UHI phenomenon, accurately determining its spatial intensity remains a challenge due to insufficient data or the limited spatial distribution of available measurements (Szymanowski, Kryza 2009). A review of the literature indicates that the topic is well understood from a theoretical standpoint, across various spatial scales: macro (climate), local (urban planning and land use), and micro (building-level interventions and improving residents' quality of life) (Kleerekoper, Van Esch and Salcedo 2012; Wonorahdjo et al. 2022; Błażejczyk et al. 2014; Deilami, Kamruzzaman and Liu 2018).

The literature distinguishes three types of UHI based on the location of temperature measurement:

1. Canopy Urban Heat Island (CUHI) – refers to air temperature measured at approximately 2 m above ground level, typically within the tree canopy layer.
2. Surface Urban Heat Island (SUHI) – refers to surface-level UHI, remotely sensed as radiative land surface temperature (LST) (Li et al. 2023).
3. Subsurface UHI – refers to underground heat islands, typically requiring temperature measurements from boreholes or monitoring wells.

These three types of UHI differ in terms of their formation mechanisms and can be linked to energy exchange processes between the surface, atmosphere, and soil (Huang et al. 2020). Although air temperature (AT), which is typically measured in studies of Canopy Urban Heat Island (CUHI), is more relevant from the perspective of thermal comfort, the spatial resolution of such data is often limited due to the number and distribution of ground-based sensors. Surface temperature, or Land Surface Temperature (LST), is frequently used in UHI research because it can be derived from satellite imagery, offering broader spatial coverage and representing surface radiative temperature (Peng et al. 2022).

Radiative temperature (TR) differs from air temperature (AT) in that it is calculated based on the amount of emitted thermal (infrared) radiation. TR tends to align more closely with AT during nighttime, when materials are not reflecting solar radiation. During the day, however, due to incoming solar radiation, significant differences between AT and TR can be observed – particularly in densely urbanized areas (Ferrini et al. 2020).

Urban areas exhibit substantial microclimatic variability. Therefore, understanding the climatic characteristics of a given location also requires attention to the temporal framework of temperature measurement – whether instantaneous, hourly, or daily averages are used. The more temperature values and spatial scales are averaged, the more local variations in air temperature tend to be obscured (Peng et al. 2022).

Within the European Union, strategic recommendations have been established to counteract the development of UHIs, including indicators and monitoring methodologies that help account for the impact of UHIs on cities and their inhabitants. Pilot projects are also being conducted

in this area (Iodice et al. 2024). Researchers are attempting to measure the effectiveness of mitigation strategies, such as urban greening and the implementation of green roofs (Błażejczyk, Błażejczyk 2023). However, challenges arise when attempting to generalize the results of pilot studies to other urban contexts. Due to varying conditions and the specific characteristics of each location, the UHI effect must be studied individually in each city (Iodice et al. 2024).

The literature identifies several key factors contributing to the UHI effect:

1. Absorption of shortwave solar radiation due to the low albedo of urban materials, which reduces reflectivity. This effect is amplified by multiple reflections between building façades and street surfaces.
2. Air pollution in the urban atmosphere, which absorbs and re-emits longwave radiation back into the urban environment.
3. Urban street canyons (building geometry): the height-to-width ratio of buildings and streets influences sky view factor – reduced sky exposure lowers heat loss via long-wave radiation. Reflected heat is reabsorbed or re-radiated back into the urban fabric.
4. Anthropogenic heat release, resulting from combustion processes such as vehicular traffic, space heating, and industrial activity.
5. Increased heat storage by building materials with high heat capacity. Additionally, urban areas have a greater surface area than rural areas, allowing them to store more heat.
6. Reduced evapotranspiration in cities due to the prevalence of impervious surfaces and lower vegetation cover compared to rural areas. This leads to higher surface and air temperatures and less atmospheric moisture.
7. Lower wind speeds in urban areas, which reduce the transport of heat out of street canyons (Kleerekoper, Van Esch and Salcedo 2012).

The collection of data on the above-mentioned factors influencing UHI and their development into urban indicators may serve as a foundation for formulating planning guidelines within a GIS system. GIS (Geographic Information System) is a tool used for collecting, managing, and analyzing spatial data, including data related to UHI. It integrates various types of data, enabling the analysis of spatial locations and the organization of information layers that can be visualized through maps and three-dimensional scenes. Point data (measurements), when processed using different algorithms, are enriched with additional information. This form of visualization facilitates data interpretation and supports planning decision-making (Ramasubramanian, Albrecht and De Leon Rojas 2024). In practice, however, not all of the factors listed above may be subject to GIS-based analysis due to the lack of local data or the absence of clear parameterization methods based on existing datasets.

One of the commonly used tools for monitoring the UHI effect is satellite imagery. These images allow for visualizing the phenomenon on a large spatial scale; however, they also have certain limitations. Temperature is represented in the form of a grid with cell sizes ranging from 30 m to

1 km, depending on the satellite data source. For instance, Landsat imagery provides a resolution of 30 m (Deilami, Kamruzzaman and Liu 2018). The measurements capture surface radiative temperature, which can be disrupted or rendered unobservable due to atmospheric conditions such as cloud cover. Depending on the satellite and its orbital parameters, data is typically collected once every 1 to 16 days at a fixed time of day (Deilami, Kamruzzaman and Liu 2018). In the case of Wrocław, measurements are acquired approximately every 7 days around 9:30 AM. As a result, publicly available datasets rarely offer imagery during nighttime hours, when the UHI effect is most pronounced due to the slower cooling of urban areas and faster cooling of rural surroundings. During daytime, the temperature contrast between urban and non-urban surfaces is significantly lower (EPA 2025).

In the reviewed scientific studies on phenomena related to UHI, satellite data were combined with urban factors using various methods and for different purposes, such as identifying relationships, determining the scale of impact, or developing development scenarios that account for UHI. Surface temperature data were typically presented in the form of grid-based datasets. Land use data were also visualized as grids, within which parameters were aggregated, allowing for direct comparison with satellite-derived temperature data. To examine the relationship between temperature and land use, grids of various resolutions were employed – for example, 2-meter grids were used in simulations with the InVEST 3.8.7 Urban Cooling Model (Zawadzka, Harris and Corstanje 2021). To investigate the influence of specific urban factors on temperature (e.g., how an increase in a given urban parameter affects the thermal characteristics of an area, or how green areas contribute to

urban cooling), grid sizes of 30 m, 60 m, 90 m, 120 m, 150 m, 180 m, 210 m, and 240 m were applied (Dai, Guldmann and Hu 2018). In studies focusing on metropolitan areas, a coarser 500 m × 500 m grid was used (Zardo et al. 2017). The analyses revealed significant correlations between urban factors and surface temperature, and proposed counteracting scenarios for the UHI effect based on the intensity of those factors. These scenarios addressed both urban-scale actions on the periphery and building-scale interventions in central areas where UHI effects are already present (Wang et al. 2024). In the case of Wrocław, an UHI Report was developed (IETU 2021), which identified zones exposed to the occurrence of surface-level UHI. However, the report did not examine the relationship between adjacent land use patterns and temperature distribution, nor did it analyze the detailed urban factors discussed below.

## Methods

### *Selection of areas for detailed analysis*

The UHI Report for Wrocław (IETU 2021) was used to identify contrasting locations – relatively cool/optimal and hot zones – exhibiting varying degrees of exposure to the UHI effect. Four locations were selected for analysis: two situated in highly urbanized surroundings, characterized by dense development and large impervious surface areas (Przedmieście Oławskie, Przedmieście Świdnickie), and two located in greener settings, in close proximity to the river and with lower building density (Olimpia Port, Plac Grunwaldzki) (see Fig. 1, Table 1). For the GIS analyses, each selected location was delineated as a territory approximately 1.2 km × 1.2 km in size.

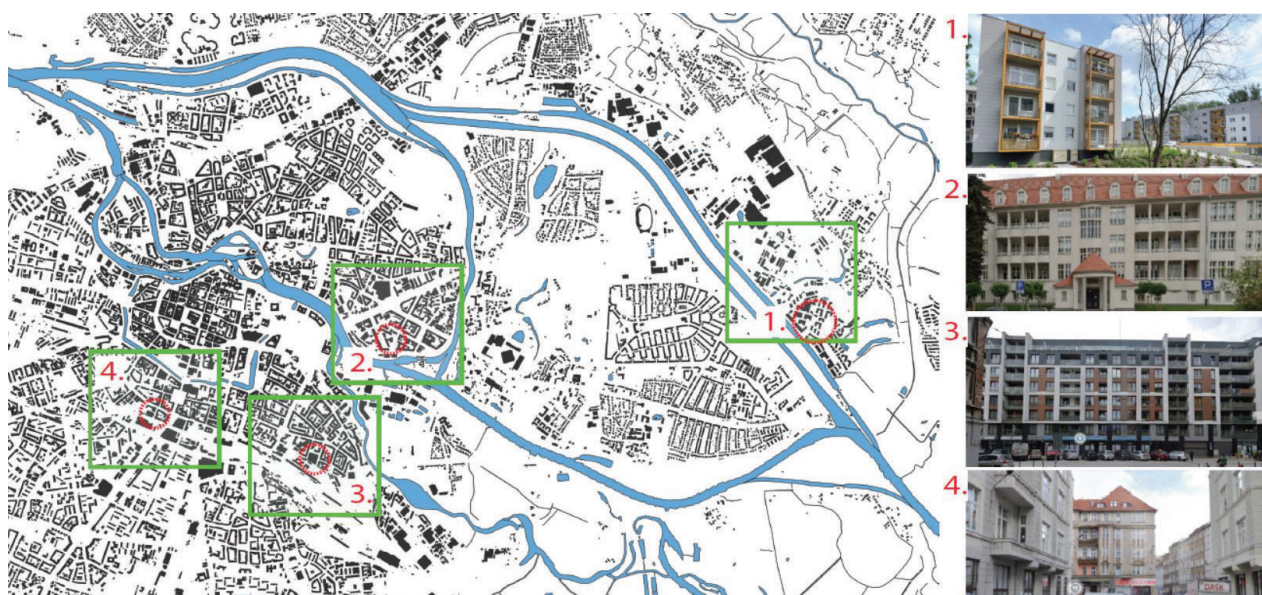


Fig. 1. Location of residential areas analyzed using GIS (green frame), location of air temperature sensors (red frame), and photographs of sample buildings where sensors were installed: 1 – Olimpia Port, 2 – Plac Grunwaldzki, 3 – Przedmieście Oławskie, 4 – Przedmieście Świdnickie (elaborated by M. Smektała)

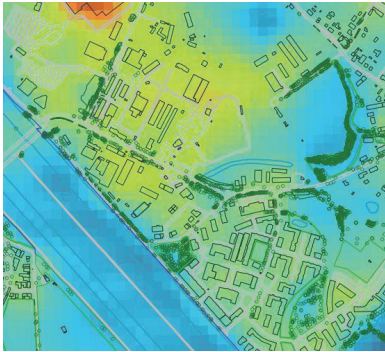
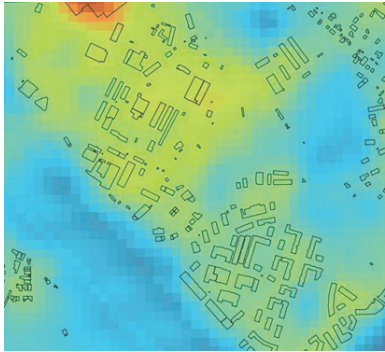
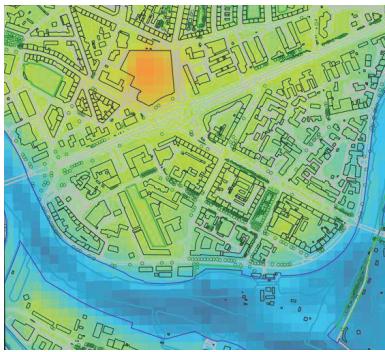
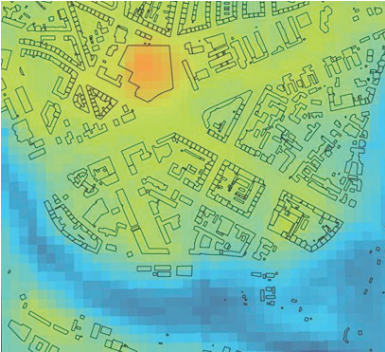
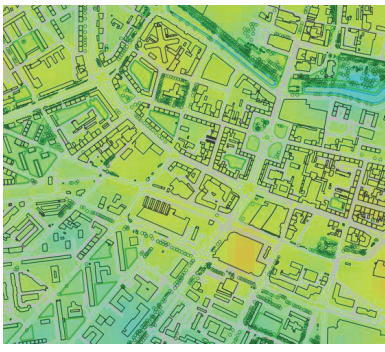
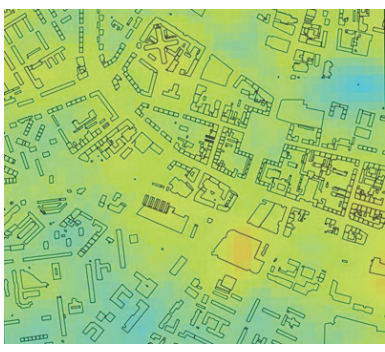
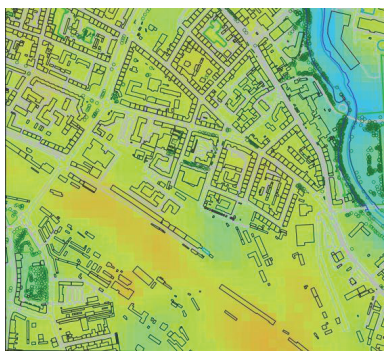
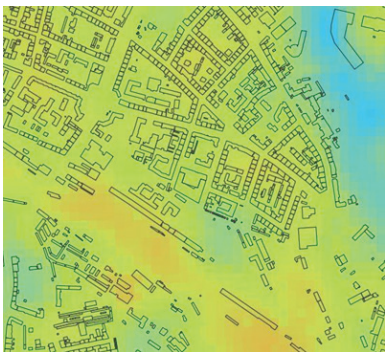
Il. 1. Lokalizacja osiedli badanych z wykorzystaniem analizy GIS (zielona ramka), lokalizacja czujników temperatury powietrza (czerwona ramka) oraz fotografie przykładowych budynków, na których zostały zamontowane czujniki: 1 – Olimpia Port, 2 – Plac Grunwaldzki, 3 – Przedmieście Oławskie, 4 – Przedmieście Świdnickie (oprac. M. Smektała)

Table 1. Overview of selected study areas. Distribution of radiative temperature in the selected areas on July 8, 2023, at 9:44 AM

(source: USGS, <https://earthexplorer.usgs.gov>)

Tabela 1. Zestawienie wybranych obszarów do badań. Rozkład temperatury radiacyjnej na wybranych obszarach z 8 lipca 2023, godz. 9:44

(źródło: USGS, <https://earthexplorer.usgs.gov>)

Range of radiative temperatures [°C]		<div> <div>57,5°C</div> <div>50°C</div> <div>45°C</div> <div>40°C</div> <div>35°C</div> <div>30°C</div> <div>26,5°C</div> </div> <div>1 pixel = 30m × 30m</div>	
Type/name of the study area		LST image with overlaid building footprints, streets, low vegetation, trees, and water surfaces (1.2 km × 1.2 km)	LST map with building outlines (1.2 km × 1.2 km)
Cool study area	Osiedle Olimpia Port		
	Plac Grunwaldzki		
Hot study area	Przedmieście Świdnickie		
	Przedmieście Oławskie		

### *Data used in the analyses – radiative temperature*

For each of the selected locations, maps depicting radiative temperature were obtained from Landsat 8 satellite imagery downloaded from the United States Geological Survey (USGS 2024). These maps represent Land Surface Temperature (LST), which primarily depends on material albedo, vegetation cover, and soil moisture. From a climatic perspective, LST is a key variable for evaluating land-atmosphere exchange processes, constraining surface energy budgets and model parameters, and providing observations of surface temperature changes both globally and in critical regions (Global Climate Observing System 2025).

The data used refer to July 8, 2023, at 9:44 AM. According to measurements from the Wrocław-Starachowice station (IMGW 2023), this was one of the hottest days of the year, with a maximum air temperature of 30.40°C, an average temperature of 22.30°C, and a minimum temperature recorded that day of approximately 11.20°C. At the time the satellite images were taken, cloud cover was minimal, ensuring complete data coverage of radiative temperature for the entire study area.

The average radiative temperature from satellite imagery is presented in a 30 × 30 m grid, with a color spectrum indicating temperature intensity. For each study area, based on zonal statistics, the following temperature metrics are calculated: mean, median, minimum, and maximum.

### *Data used in the analyses – urban factors database*

To identify the relationships influencing the UHI effect, radiative temperature from Landsat 8 imagery was compared with a custom-developed database of urban factors potentially affecting air temperature in the city. Based on data provided by the Municipality of Wrocław Office, information was collected to derive urban indicators including: built-up area, building volume, and average building height, as well as green area, green volume, and average vegetation height. These indicators are commonly used by researchers to calculate the so-called “roughness” coefficient. Roughness is linked to the assessment of urban ventilation potential and, consequently, the area’s natural capacity for cooling or heating (Wang et al. 2024).

To allow comparison of Landsat data with selected urban indicators and to enable comparisons across study areas on a city-wide scale, the indicators derived from building and vegetation datasets were represented on a 30 × 30 m grid (Zawadzka, Harris and Corstanje 2021; Dai, Guldmann and Hu 2018), calibrated to match the Landsat 8 grid with high spatial accuracy. Table 2 presents the types of indicators, the method of their calculation, and the format of the resulting data.

The greenery dataset consists of raster data with a resolution of 3 × 3 m, derived from LiDAR data for the city of Wrocław. These data represent the actual surface area and height of vegetation across the entire urban area. The dataset was processed using a zonal statistics algorithm, which calculated the number of raster pixels representing vegetated surfaces of varying heights within each grid cell. Based on this information, the vegetation cov-

er area, volume, and average height were computed for each cell of the grid. The total green area was determined by projecting vegetated objects onto the ground surface. This approach accounts for both low vegetation such as grass and the canopy projection of trees onto sidewalks. The building dataset is a vector dataset containing various attributes of buildings, including footprint area, height, function, and year of construction. To facilitate further analysis, these data were transformed into a 30 × 30 m grid. For each building segment within a grid cell, the footprint area was calculated. Polygon data were converted into centroids, which retained all associated building attributes (e.g., height, function). These centroid data were then aggregated within each grid cell. As a result, three key indicators were derived for each 30 × 30 m grid cell: total building footprint area (sum of built-up area in [m<sup>2</sup>]), total building volume (sum of built-up volume in [m<sup>3</sup>]), and average building height (mean building height in [m]).

## **Results**

The results of the conducted analyses can be categorized into two types: general results comparing the study areas with one another, and detailed results concerning the impact of individual factors on LST. The general results include indicators related to buildings, greenery, and radiative temperature (Table 3). These indicators were used to construct a profile for each area, based on various parameters that allow for comparative analysis.

The highest average radiative temperature was recorded in the Przedmieście Oławskie area, reaching 42.7°C. This area also has the lowest green surface coverage. A slightly lower average temperature of 41.2°C was observed in Przedmieście Świdnickie, which features the highest building footprint and volume indicators. Compared to Przedmieście Oławskie, Przedmieście Świdnickie has a greater extent of green areas. The lowest temperature, 29.2°C, was recorded in the Plac Grunwaldzki neighborhood, specifically in the grid cells overlapping with the Odra River. The lowest average temperature, 37.8°C, was noted in the Olimpia Port neighborhood, where over 50% of the area is covered by vegetation. However, the highest temperature overall – 52.7°C – was also observed in Olimpia Port, but in its industrial zone, outside the residential area. As seen in previous examples, areas with high building indicators show a noticeable cooling effect in the presence of water bodies and vegetation.

Within the studied areas, the strongest correlation with average temperature was observed for parameters related to the surface area and volume of greenery, which at this scale appears to play a significant role in lowering the mean temperature. A high correlation was also found between indicators related to building footprint and volume and temperature. There is a clear inverse correlation between greenery-related indicators and both temperature and built-up area.

To better understand these correlations and the characteristics of specific city sections, it is necessary to examine the spatial distribution of temperature on maps that provide the contextual background of the analyzed factors (Tables 4, 5).

Table 2. Summary and specification of urban metrics (elaborated by K. Lewacki)  
 Tabela 2. Zestawienie i charakterystyka wskaźników urbanistycznych (oprac. K. Lewacki)

No.	Urban indicator	Input data	Processing method	Output data	Area parameters
1	Build-up area	Vector data	aggregating values into grid cells	grid 30 × 30 m	building footprint area percentage, mean size within the grid cell
2	Mean building height				average building height
3	Building volume				building volume for the area, mean size within the grid cell
4	Greenery area	grid 3 × 3 m	zonal statistics		greenery area percentage, mean size within the grid cell
5	Mean green height				average greenery height
6	Greenery volume				geenery volume for the area, mean size within the grid cell

Table 3. Urban and temperature indicators – results for the study areas (elaborated by K. Lewacki)  
 Tabela 3. Wskaźniki urbanistyczne i temperaturowe – wyniki dla badanych obszarów (oprac. K. Lewacki)

Urban and temperature Indicators		Olimpia Port	Plac Grunwaldzki	Przedmieście Świdnickie	Przedmieście Oławskie
Building footprint	Average building footprint area [m <sup>2</sup> in a grid of 900 m <sup>2</sup> ]	85.85	185.93	215.63	205.98
	Total building footprint area [m <sup>2</sup> ]	137280.50	298053.44	345013.21	329563.24
	Percentage of building footprint area [%]	9.53	20.70	23.96	22.89
	Mean building volume area [m <sup>3</sup> per 900 m <sup>2</sup> plot]	749.93	2976.59	3976.20	2891.01
	Total building volume [m <sup>3</sup> ]	1199133	4771480	6361916	4625614
	Average building height [m]	8.20	15.25	17.61	12.84
Greenery	Average greenery area [m <sup>2</sup> in a grid of 900 m <sup>2</sup> ]	474.06	361.71	350.63	313.01
	Total greenery area [m <sup>2</sup> ]	758028	579825	561008	500819
	Percentage of greenery area [%]	52.64	40.27	38.96	34.78
	Average greenery volume [m <sup>3</sup> in a grid of m <sup>2</sup> ]	2355.06	2140.45	2030.15	1437.99
	Total greenery volume [m <sup>3</sup> ]	3737479	3242787	3177192	2273458
	Mean greenery height [m]	3.85	4.40	4.31	3.31
Radiative temperature [°C]	Average	37.80	38.89	41.15	42.72
	Median	37.77	40.01	41.21	43.18
	The lowest	31.56	29.17	35.47	34.27
	The highest	52.70	48.93	46.19	46.95
	Value range	21.14	19.76	10.73	12.67
	Variance (measure of dispersion around the mean)	11.97	16.07	3.55	4.97
Legend:					
	Value of the given indicator related to temperature and built-up area	Low	Mean	High	The highest
	Value of the given indicator related to greenery	Low	Mean	High	The highest

Table 4. Summary of Land Surface Temperature (LST) with selected urban indicators describing the built environment of the four analyzed areas measuring  $1.2 \times 1.2$  km. Internal grid:  $30 \times 30$  m (elaborated by K. Lewacki, M. Smektała)  
 Tabela 4. Zestawienie LST z wybranymi wskaźnikami urbanistycznymi opisującymi zabudowę czterech analizowanych obszarów o wymiarach  $1.2 \times 1.2$  km. Wewnętrzna siatka:  $30 \times 30$  m (oprac. K. Lewacki, M. Smektała)

		Radiative temperature [°C]	Building footprint area percentage [%]	Building footprint area [m <sup>2</sup> ]	Building height [m]	Building volume [m <sup>3</sup> ]
Legend		<p>57,5°C 50°C 45°C 40°C 35°C 30°C 26,5°C</p>	<p>0 - 3,8 3,8 - 11,5 11,5 - 19,7 19,7 - 28,3 28,3 - 37,3 37,3 - 46,7 46,7 - 57,6 57,6 - 71,5 71,5 - 88,4 88,4 - 100</p>	<p>0 - 34 34 - 104 104 - 177 177 - 255 255 - 336 336 - 420 420 - 519 519 - 643 643 - 796 796 - 900</p>	<p>✓ 0 - 1 ✓ 1 - 5 ✓ 5 - 8 ✓ 8 - 11 ✓ 11 - 14 ✓ 14 - 18 ✓ 18 - 22 ✓ 22 - 28 ✓ 28 - 39 ✓ 39 - 56</p>	<p>0 - 545 545 - 1672 1672 - 3009 3009 - 4738 4738 - 6869 6869 - 9276 9276 - 12335 12335 - 16336 16336 - 23212 23212 - 35377</p>
Cool area	Olimpia Port					
	Plac Grunwaldzki					
Hot area	Przedmieście Oławskie					
	Przedmieście Świdnickie					

For example, the southern part of Przedmieście Świdnickie features more greenery combined with lower building density, which significantly reduces radiative temperature compared to other parts of the neighborhood – by as much as 7°C in some areas. Conversely, higher temperature values, exceeding 42°C, prevail in highly urbanized zones of this neighborhood. Elevated temperatures are also noticeable in closed urban blocks, where the difference compared to open urban layouts is approximately 3°C.

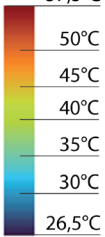
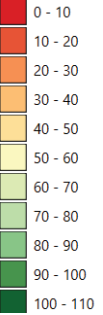
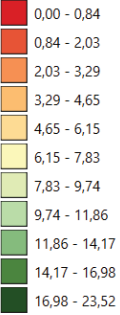
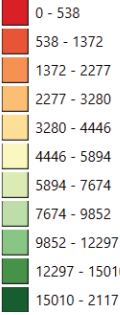
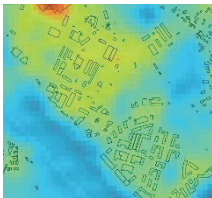
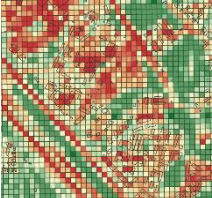
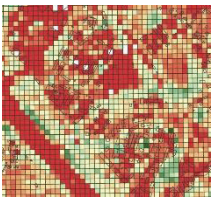
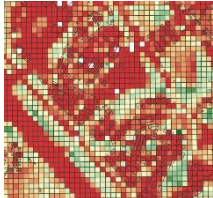
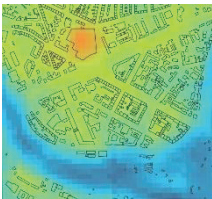
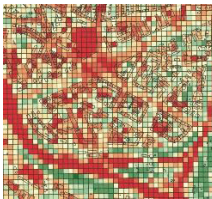
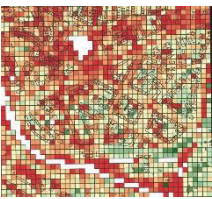
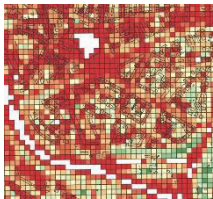
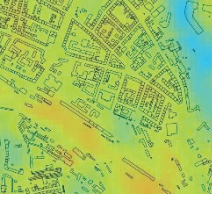
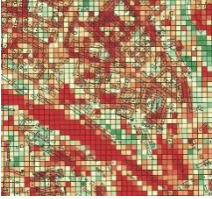
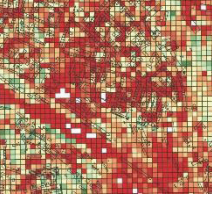
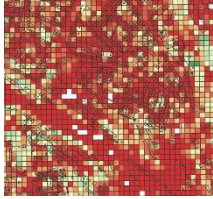
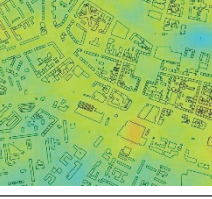
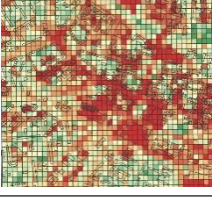
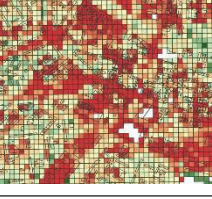
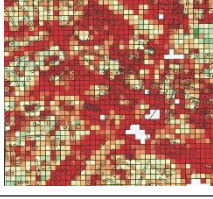
In Olimpia Port, characterized by a low average area temperature, the highest temperature of 52.6°C was simultaneously recorded. This localized high temperature occurs in industrial zones with a high percentage of built-up area, while the building volume index remains at a moderate level. In other parts of this area, where building volume

and coverage indicators are high but dispersed, no significant increase in radiative temperatures was observed. High radiative temperatures are also exhibited by large commercial buildings in Przedmieście Świdnickie and Plac Grunwaldzki, despite their proximity to rivers or moats. Plac Grunwaldzki is characterized by relatively dense development; however, the presence of water, greenery, and wide profiles of main streets cools the area by 3°C to 8°C.

In Przedmieście Oławskie, it is noteworthy that the highest radiative temperature was recorded in railway areas with very low built-up coverage and low building volume indices.

The results obtained from the indicator analysis suggest that further research requires the collection of more detailed data. Discrepancies were observed between the relationship of average temperature and building-related

Table 5. Summary of Land Surface Temperature (LST) with selected urban indicators describing greenery within the four analyzed areas measuring  $1.2 \times 1.2$  km. Internal grid:  $30 \times 30$  m (elaborated by K. Lewacki, M. Smektała)  
 Tabela 5. Zestawienie LST z wybranymi wskaźnikami urbanistycznymi opisującymi zieleń w ramach czterech analizowanych obszarów o wymiarach  $1.2 \times 1.2$  km. Wewnętrzna siatka:  $30 \times 30$  m (oprac. K. Lewacki, M. Smektała)

		Radiative temperature [°C]	Percentage of greenery area [%]	Greenery height [m]	Greenery volume [m <sup>3</sup> ]
Legend		 57,5°C 50°C 45°C 40°C 35°C 30°C 26,5°C	 0 - 10 10 - 20 20 - 30 30 - 40 40 - 50 50 - 60 60 - 70 70 - 80 80 - 90 90 - 100 100 - 110	 0,00 - 0,84 0,84 - 2,03 2,03 - 3,29 3,29 - 4,65 4,65 - 6,15 6,15 - 7,83 7,83 - 9,74 9,74 - 11,86 11,86 - 14,17 14,17 - 16,98 16,98 - 23,52	 0 - 538 538 - 1372 1372 - 2277 2277 - 3280 3280 - 4446 4446 - 5894 5894 - 7674 7674 - 9852 9852 - 12297 12297 - 15010 15010 - 21171
Cool area	Olimpia Port				
	Plac Grunwaldzki				
Hot area	Przedmieście Oławskie				
	Przedmieście Świdnickie				

indicators. Therefore, it is reasonable to expand the indicator base, for example, by including data related to soil permeability and construction materials.

### Discussion

The literature studies on the UHI effect have addressed various scales and aspects of the phenomenon, yet often without integrating these perspectives or analyzing their interrelationships. At the macro scale, Wrocław is located in a climatic zone favorable for leveraging cooling through ventilation, including so-called nighttime cooling (Artmann et al. 2008). However, the effectiveness of nighttime cooling depends, among other factors, on the local intensity of the atmospheric UHI effect, which is illustrated by the

variation in the number of tropical nights during the summer of 2024, ranging from 2 to 31 across different parts of the city (Baborska-Narożny, Kostka and Smektała 2024).

In contrast, studies on surface-level UHI at smaller scales have typically focused on the influence of isolated urban factors – such as greenery or buildings – on land surface temperature (Wang et al. 2024; Zawadzka, Harris and Corstanje 2021; Dai, Guldmann and Hu 2018). Two major challenges hinder the development of studies linking urban morphology parameters with LST: the lack of sufficiently detailed data on the analyzed factors, and the absence of established methodologies for assessing their mutual interactions.

The results presented in this article indicate that identifying relationships between these factors is crucial to miti-

gating the surface UHI effect and forming a basis for urban planning guidelines. The method proposed here confirms findings available in the existing literature, yet by incorporating a greater number of urban variables, it enables a more refined understanding of the issue – for example, by allowing the cooling effect of green spaces to be estimated in the context of surrounding urban morphology.

GIS data are increasingly being used in policymaking for cities aiming to enhance resilience against heatwaves. These cities focus primarily on identifying hotspots and directing greening or cooling corridor interventions toward them (Musco 2016; ClimateADAPT 2025). Researchers studying the UHI effect emphasize the relevance of surface permeability and vegetation height indicators in determining the cooling potential of green areas, as these tend to exhibit lower air temperatures (Kuchcik, Czarnecka and Błażejczyk 2024). It is examined that green spaces larger than 2 ha can contribute to urban cooling, and the spatial reach of this effect is linked to vegetation height. It is estimated that the horizontal cooling impact of greenery extends up to five times the height of the trees (Zardo et al. 2017).

In the case of Wrocław, preliminary results for selected areas show that building density and height can increase radiative temperatures by up to 5°C, while proximity to water and greenery can reduce them by about 7°C compared to the hottest areas. Radiative temperatures in densely built-up areas range from 42°C to 46°C, while similarly dense zones adjacent to green spaces or rivers show temperatures ranging from 35°C to 42°C. The cooling influence of the river can extend up to 350 m into the urban fabric.

Based on the analyses presented in this article, it is evident that the extent of the river's cooling effect is also influenced by other urban factors. The findings suggest that this effect is not uniform – there are observable relationships with building-related indicators. Compared to the UHI Report for Wrocław (IETU 2021), this study develops a database incorporating a broader set of urban variables represented as grid-based data. Identifying a larger number of interrelations enables a deeper understanding of the causes and mitigation of the UHI effect, and supports the development of typologies for different urban areas. Nonetheless, a more comprehensive understanding of UHI still requires expanding the diversity and granularity of the factors studied.

For cities, it is essential to develop future development scenarios based on an understanding of the relationship between the local intensity of the UHI phenomenon – both surface and atmospheric – and urban form indicators. The literature provides examples where LST analyses have been compared with air temperature measurements (Hartz et al. 2006). However, until now, the ability to verify and compare surface and atmospheric UHI effects at the city scale has been considered limited due to the insufficient number of air temperature measurement points (Gawuć et al. 2020). Improved knowledge of the interconnections between different types of the UHI effect would enable more precise formulation of guidelines for mitigating or preventing UHI. Such guidelines could be applied at multiple scales – from urban planning strategies (e.g., green space allocation) to building-level interventions (e.g., typologies that support natural ventilation or nighttime cooling).

The GIS-based analytical method proposed in this article can support visualization of the relationship between elevated radiative temperatures and the urban factors that contribute to their increase. Further development of this method could enable its application in determining optimal locations for air temperature monitoring stations. Verifying the influence of urban form indicators in relation to air temperature profiles would make it possible to generalize data from selected measurement points, allowing for extrapolation to other urban areas with similar characteristics.

## Conclusions

This article presents a GIS-based methodology for analyzing high-resolution urban morphology data provided by the City of Wrocław. By integrating radiative temperature measurements derived from Landsat 8 imagery captured around 9:00 a.m. with a suite of urban indicators – namely footprint area, built volume, and mean height for both buildings and vegetation – mapped on a uniform 30 × 30 m grid, we reveal interdependencies between these indicators and the surface UHI effect. The study workflow comprised two analytical levels. First, general comparisons across multiple study areas identified broad relationships between urban-form metrics and radiative temperature. Second, detailed within-area analyses at the same grid resolution determined the spatial scales at which particular factors exert the most influence. This dual approach allowed us to pinpoint threshold values of environmental parameters that either exacerbate or mitigate surface warming. The proposed method simplifies complex vector and raster data into comparable grid-cell summaries, enabling the classification of city blocks by their indicator profiles. By matching areas with similar urban-form signatures, we can test whether they exhibit analogous radiative temperature distributions. Where discrepancies arise, further GIS analyses can explore additional variables – such as material emissivity, façade color, or street-canyon geometry – to explain residual thermal variation. Finally, we note that instantaneous radiative temperature maps do not directly represent air temperature. For a comprehensive assessment of nighttime cooling potential during heatwaves, these surface data should be supplemented with in-situ air temperature measurements.

Within the analyses, we quantified the influence of individual indicators on land surface (radiative) temperature and described these relationships at different spatial scales. At the broader scale, the most significant drivers of average temperature were the area of vegetation and the area of built fabric. At the finer scale, building height – and the spatial configuration of building footprint and volume – became more important. In such contexts, clusters with high values of these indicators corresponded to pronounced temperature increases.

Our results show that high-canopy vegetation cover substantially reduces surface temperature. This cooling effect also applies in built-up zones, provided that built-up clusters are not contiguous but interspersed with greenery. While vegetation volume and height have a lesser impact on absolute temperature reduction, they modulate the spatial extent of the cooling effect. We further assessed the reach of high-canopy

cooling, finding it to be heterogeneous and dependent not only on the area of tree cover but also on surrounding building parameters – especially vegetation volume and height.

Importantly, we identified sections of the Przedmieście Oławskie rail yards where both vegetation and building indicators are low, yet where the highest radiative temperatures were recorded. We also observed that areas with the lowest mean temperatures exhibited the greatest temperature ranges – that is, despite a low average, they experienced both the lowest and highest extremes among all study sites.

Scaling up the GIS-based method presented here could inform urban-planning guidelines – such as prescribing

maximum building densities or minimum high-canopy green cover to mitigate the Urban Heat Island effect. For a comprehensive depiction of urban form's influence on ambient temperature, future studies should incorporate additional indicators – street canyons and airflow, impervious surface fraction, building materials, wind direction and speed – as well as surface-temperature data from times other than morning overpasses and in situ air-temperature measurements at the building scale.

Translated by  
Marta Smechtala

### Acknowledgements

The Authors acknowledge voluntary assistance of individuals and institutions (Wrocław Municipality, Faculty of Mathematics – Wrocław TECH), KADRA Szkoła Policealna, Chilli Hostel) who provided ac-

cess to their buildings. This research was supported by Wrocław TECH funding granted as part of Accademia Professorum Iuniorum Grant Nr 50AP/0001/24.

### References

- Artmann, Nikolai, Dimitrios Gyalistras, Heinrich Manz, and Per Heiselberg. "Impact of Climate Warming on Passive Night Cooling Potential." *Building Research and Information* 36, no. 2 (2008): 111–28. <https://doi.org/10.1080/09613210701621919>.
- Baborska-Narożny, Magdalena, Maria Kostka, and Marta Smechtala. "Informing Housing Planning Policy to Minimize the Need for Active Cooling in Temperate (Cfb) Climate." In *Comfort at the Extremes 2024 – Investing in Well-Being in a Challenging Future. Proceedings of 2024 CATE*, edited by Jessica Fernández-Agüera, Samuel Domínguez-Amarillo, and Susan Roaf. Seville, [2024]. [Accepted for forthcoming publication].
- Błażejczyk, Krzysztof, and Anna Błażejczyk. "Zmiany klimatu i ich wpływ na budownictwo i komfort życia mieszkańców miast, przykład Warszawy." *Przegląd Geograficzny* 68, no. 1–2 (2023): 29–53. <https://doi.org/10.32045/PG-2023-036>.
- Błażejczyk, Krzysztof, Magdalena Kuchcik, Paweł Milewski, et al. *Miejska wyspa ciepła w Warszawie: Uwarunkowania klimatyczne i urbanistyczne*. Instytut Geografii i Przestrzennego Zagospodarowania PAN, Wydawnictwo Akademickie SEDNO, 2014.
- Błażejczyk, Krzysztof, Robert Twardosz, Piotr Wałach, Kaja Czarnecka, and Anna Błażejczyk. "Heat Strain and Mortality Effects of Prolonged Central European Heat Wave – an Example of June 2019 in Poland." *International Journal of Biometeorology* 66, (2022): 149–61. <https://doi.org/10.1007/s00484-021-02202-0>.
- Buguet, Alain, Manny W. Radomski, Jacques Reis, and Peter S. Spencer. "Heatwaves and Human Sleep: Stress Response versus Adaptation." *Journal of the Neurological Sciences* 454, (November 2023): 120862. <https://doi.org/10.1016/j.jns.2023.120862>.
- ClimateADAPT. "Enhancing Social Justice in Actions to Adapt to Climate Change in the City of Barcelona" (2025). Accessed June 6, 2025, at <https://climate-adapt.eea.europa.eu/en/metadata/case-studies/barcelona-trees-tempering-the-mediterranean-city-climate>.
- Dai, Xiaoxin, Jean-Michel Guldmann, and Yunfeng Hu. "Spatial Regression Models of Park and Land-Use Impacts on the Urban Heat Island in Central Beijing." *Science of The Total Environment* 626, (June 2018): 1136–47. <https://doi.org/https://doi.org/10.1016/j.scitotenv.2018.01.165>.
- Deilami, Kaveh, Md. Kamruzzaman, and Yan Liu. "Urban Heat Island Effect: A Systematic Review of Spatio-Temporal Factors, Data, Methods, and Mitigation Measures." *International Journal of Applied Earth Observation and Geoinformation* 67, (May 2018): 30–42. <https://doi.org/10.1016/j.jag.2017.12.009>.
- Dubicki, Alfred, Maria Dubicka, and Mariusz Szymanowski. "Klimat Wrocławia." In *Informator o stanie środowiska Wrocławia 2002*, edited by Krzysztof Smolnicki and Mariusz Szykasiuk, Dolnośląska Fundacja Ekorozwoju, Gmina Wrocław, 2002.
- Eliasson, Ingegard, and Marie Svensson. "Spatial Air Temperature Variations and Urban Land Use – A Statistical Approach." *Meteorological Applications* 10, no. 2 (2003): 135–49. <https://doi.org/10.1017/S1350482703002056>.
- EPA. "What are Heat Islands? US EPA." Last updated April 3, 2025. Accessed June 11, 2025, at <https://www.epa.gov/heatislands/what-are-heat-islands>.
- Ferrini, Francesco, Alessio Fini, Jacopo Mori, and Antonella Gori. "Role of Vegetation as a Mitigating Factor in the Urban Context." *Sustainability* 12, no. 10 (2020): 4247. <https://doi.org/10.3390/su12104247>.
- Gawuś, Lech, Karol Paweł Szymankiewicz, Maciej Krystian Jefimow, et al. "Statistical Modeling of Urban Heat Island Intensity in Warsaw, Poland Using Simultaneous Air and Surface Temperature Observations." *IEEE Journal of Selected Topics in Applied Earth Observations and Remote Sensing* 13 (2020), 2716–28. <https://doi.org/10.1109/JSTARS.2020.2989071>.
- Global Climate Observing System. "Land Surface Temperature." Accessed April 17, 2025, at <https://gcos.wmo.int/site/global-climate-observing-system-gcos/essential-climate-variables/land-surface-temperature>.
- Hartz, Donna, Lela Prashad, Brent Hedquist, Jay Golden, and Anthony Brazel. "Linking Satellite Images and Hand-Held Infrared Thermography to Observed Neighborhood Climate Conditions." *Remote Sensing of Environment* 104, no. 2 (2006): 190–200. <https://doi.org/10.1016/j.rse.2005.12.019>.
- Huang, Fan, Wenfeng Zhan, Zhi Hua Wang, et al. "Satellite Identification of Atmospheric-Surface-Subsurface Urban Heat Islands under Clear Sky." *Remote Sensing of Environment* 250 (2020), 112039. <https://doi.org/10.1016/j.rse.2020.112039>.
- IEA. "Tracking Clean Energy Progress 2023." Published July, 2023. Accessed June 6, 2025, at <https://www.iea.org/reports/tracking-clean-energy-progress-2023>.
- IETU. "Opracowanie dotyczące występowania powierzchniowej miejskiej wyspy ciepła dla obszaru miasta Wrocław." Published 2021. Accessed June 11, 2025, at <https://bip.um.wroc.pl/arttykul/1081/64691/miejska-wyspa-ciepła-dla-obszaru-miasta-wrocław>.
- IMGW. "Charakterystyka wybranych elementów klimatu w Polsce w 2023 roku – podsumowanie." Published January 23, 2024. Accessed June 6, 2025, at <https://www.imgw.pl/wydarzenia/charakterystyka-wybranych-elementow-klimatu-w-polsce-w-2023-roku-podsumowanie>.
- IMGW. "Index of /data/dane\_pomiarowo\_obserwacyjne/dane\_meteorologiczne/dobowe/synop/2023" (2023). Last modified January 31, 2024. Accessed June 6, 2025, at [https://danepubliczne.imgw.pl/data/dane\\_pomiarowo\\_obserwacyjne/dane\\_meteorologiczne/dobowe/synop/2023/](https://danepubliczne.imgw.pl/data/dane_pomiarowo_obserwacyjne/dane_meteorologiczne/dobowe/synop/2023/).

- Iodice, Silvia, Luca Arbau, Antigoni Maistralli, et al. "EU Cities and Heat Extremes." European Commission, Ispra, 2024, JRC13789. Accessed June 11, 2025, at <https://publications.jrc.ec.europa.eu/repository/handle/JRC137891>.
- Jessel, Sonal, Samantha Sawyer, and Diana Hernández. "Energy, Poverty, and Health in Climate Change: A Comprehensive Review of an Emerging Literature." *Frontiers in Public Health* 7 (December 2019). <https://doi.org/10.3389/fpubh.2019.00357>.
- Kleerekoper, Laura, Marjolein Van Esch, and Tadeo Baldiri Salcedo. "How to Make a City Climate-Proof, Addressing the Urban Heat Island Effect." *Resources, Conservation and Recycling* 64 (July 2012): 30–8. <https://doi.org/10.1016/j.resconrec.2011.06.004>.
- Kuchcik, Magdalena, Kaja Czarnecka, and Krzysztof Błażejczyk. "Urban Climate Urban Heat Island in Warsaw (Poland): Current Development and Projections for 2050." *Urban Climate* 55, (April 2024). <https://doi.org/10.1016/j.uclim.2024.101901>.
- Li, Zhao Liang, Hua Wu, Si Bo Duan, et al. "Satellite Remote Sensing of Global Land Surface Temperature: Definition, Methods, Products, and Applications." *Reviews of Geophysics* 61, no. 1 (2023): 1–77. <https://doi.org/10.1029/2022RG000777>.
- Lundgren-Kownacki, Karin, Elisabeth Dalholm Hornyanszky, Tuan Anh Chu, Johanna Alkan Olsson, and Per Becker. "Challenges of Using Air Conditioning in an Increasingly Hot Climate." *International Journal of Biometeorology* 62, no. 3 (2018): 401–12. <https://doi.org/10.1007/s00484-017-1493-z>.
- Mąkosza, Agnieszka, Jadwiga Nidzgorska-Lencewicz, Czesław Koźmiński, and Bożena Michalska. "Very Warm and Tropical Nights in Voivodeship Cities in Poland in the Period 1971–2020." *Acta Geographica Lodziana* 117, (December 2024): 53–68. <https://doi.org/10.26485/AGL/2024/117/4>.
- Musco, Francesco, ed. *Counteracting Urban Heat Island Effects in a Global Climate Change Scenario*. Springer Open, 2016. <https://doi.org/10.1007/978-3-319-10425-6>.
- Pałczyński, Cezary, Izabela Kupryś-Lipinska, Tomasz Witczak, Ewa Jassem, Anna Breborowicz, and Piotr Kuna. "The Position Paper of the Polish Society of Allergy on Climate Changes, Natural Disasters and Allergy and Asthma." *Advances in Dermatology and Allergology* 35, no. 6 (2018): 552–62. <https://doi.org/10.5114/ada.2017.71273>.
- Peng, Wangchongyu, Rui Wang, Jin Duan, Weijun Gao, and Zhengxi Fan. "Surface and Canopy Urban Heat Islands: Does Urban Morphology Result in the Spatiotemporal Differences?" *Urban Climate* 42, (March 2022): 101136. <https://doi.org/10.1016/j.uclim.2022.101136>.
- Ramasubramanian, Laxmi, Jochen Albrecht, and Deborah De Leon Rojas. *GIS and Housing Principles and Practices*. Taylor & Francis, 2024.
- Runhaar, Hens, Heleen Mees, Arjan Wardekker, Jeroen van der Sluijs, and Peter P.J. Driessen. "Adaptation to Climate Change-Related Risks in Dutch Urban Areas: Stimuli and Barriers." *Regional Environmental Change* 12, (February 2012): 777–90. <https://doi.org/10.1007/s10113-012-0292-7>.
- Serwis Rzeczypospolitej Polskiej, Horyzontalny Punkt Kontaktowy Polska Centralna. "Łódź, Warszawa, Kraków, Rzeszów, Wrocław – na liście 100 ośrodków miejskich uczestniczących projekcie neutralności klimatycznej." Published May 25, 2022. Accessed June 11, 2025, at <https://www.gov.pl/web/hpkpc/lodz-warszawa-krakow-rzeszow-wroclaw---na-liscie-100-osrodkow-miejskich-uczestniczacych-projekcie-neutralnosci-klimatycznej>.
- Szymanowski, Mariusz, and Maciej Kryza. "GIS-Based Techniques for Urban Heat Island Spatialization." *Climate Research* 38, no. 2 (2009): 171–87. <https://doi.org/10.3354/cr00780>.
- Toldi, Timothée de, Salmaan Craig, and Laxmi Sushama. "Internal Thermal Mass for Passive Cooling and Ventilation: Adaptive Comfort Limits, Ideal Quantities, Embodied Carbon." *Buildings and Cities* 3, no. 1 (2022): 42–67. <https://doi.org/10.5334/bc.156>.
- USGS. "EarthExplorer" (2024). Accessed June 6, 2025. <https://earthexplorer.usgs.gov/>.
- Viguié, Vincent, Aude Lemonsu, Stéphane Hallegatte, et al. "Early Adaptation to Heat Waves and Future Reduction of Air-Conditioning Energy Use in Paris." *Environmental Research Letters* 15, no. 7 (2020): 75006. <https://doi.org/10.1088/1748-9326/ab6a24>.
- Wang, Shiang-Yu, Hsing-Yu Ou, Ping-Chun Chen, and Tzu-Ping Lin. "Implementing Policies to Mitigate Urban Heat Islands: Analyzing Urban Development Factors with an Innovative Machine Learning Approach." *Urban Climate* 55 (May 2024): 101868. <https://doi.org/10.1016/j.uclim.2024.101868>.
- WHO. "Heat and Health". Published May 28, 2024. Accessed June 6, 2025, at <https://www.who.int/news-room/fact-sheets/detail/climate-change-heat-and-health>.
- Wonorahardjo, Surjamanto, Inge Magdalena Sutjahja, Y. Mardiyati, et al. "Effect of Different Building Façade Systems on Thermal Comfort and Urban Heat Island Phenomenon: An Experimental Analysis." *Building and Environment* 217, (June 2022): 109063. <https://doi.org/10.1016/j.buildenv.2022.109063>.
- Zardo, Linda, Davide Geneletti, M. Pérez-Soba, and M. Van Eupen. "Estimating the Cooling Capacity of Green Infrastructures to Support Urban Planning." *Ecosystem Services* 26, (August 2017): 225–35. <https://doi.org/10.1016/j.ecoser.2017.06.016>.
- Zawadzka, Joanna, J.A. Harris, and Ron Corstanje. "Assessment of Heat Mitigation Capacity of Urban Greenspaces with the Use of InVEST Urban Cooling Model, Verified with Day-Time Land Surface Temperature Data." *Landscape and Urban Planning* 214, (October 2021): 104163. <https://doi.org/10.1016/j.landurbplan.2021.104163>.

## Streszczenie

### Generalizacja danych GIS jako narzędzie wspomagające rozumienie efektu miejskiej wyspy ciepła. Studium przypadku Wrocławia

Tematem artykułu jest wpływ poszczególnych czynników urbanistycznych na efekt miejskiej wyspy ciepła (MWC) oraz korelacja między tymi czynnikami. Autorzy podjęli próbę zweryfikowania możliwości wykorzystania danych systemów informacji geograficznej (GIS) do zbadania efektu MWC i w dalszych badaniach do zweryfikowania potencjału chłodzenia nocnego w mieście na przykładzie Wrocławia. W badaniu wykorzystano zdjęcia satelitarne Landsat 8 oraz dane przestrzenne dotyczące zieleni i zabudowy do przeanalizowania wpływu tych ostatnich czynników na temperaturę radiacyjną w mieście. Zaproponowana metoda umożliwia uproszczenie i kalibrację danych, co pozwala na porównywanie różnych obszarów miasta o podobnych charakterystykach. Umożliwia również sumowanie i badanie relacji wartości poszczególnych wskaźników urbanistycznych w ramach jednego pola siatki lub badanego obszaru. Dzięki temu można wyznaczyć tereny, które mają podobne zestawienia wskaźników, i porównać ich rozkłady temperatur. W przypadku różnic analizy GIS pozwalają na badanie sąsiedztwa i identyfikację innych czynników wpływających na różnice w temperaturze radiacyjnej.

Dzięki przeprowadzonym badaniom wykazano, jak poszczególne czynniki wpływają na temperaturę otoczenia. Gęstość i wysokość zabudowy znacząco podnoszą temperaturę radiacyjną, podczas gdy obecność wody i zieleni, zwłaszcza wysokiej, ma efekt chłodzący. Aby ocenić różnice w rozkładzie temperatury w przestrzeni zurbanizowanej porównano cztery lokalizacje we Wrocławiu, które różnią się intensywnością zabudowy i poziomem zazielenienia: Przedmieście Oławskie, Przedmieście Świdnickie, Plac Grunwaldzki i Olimpia Port. Wyniki wskazują, że Przedmieście Oławskie, pomimo obecności rzeki, ma najwyższą temperaturę radiacyjną z powodu gęstej zabudowy i małej ilości zieleni. W przeciwieństwie do niego, Olimpia Port, z najmniejszą gęstością zabudowy i największą ilością zieleni, jest najchłodniejszym obszarem. Celem autorów było wyznaczenie reprezentatywnych dla tkanki miejskiej obszarów, w których można przeprowadzić dalszy etap badań – pomiar lokalnej temperatury powietrza. W kolejnych fazach projektu planowane jest uwzględnienie dodatkowych czynników, takich jak przepływ powietrza, powierzchnia nieprzepuszczalna i materiały budowlane, aby bardziej szczegółowo zbadać wpływ urbanistyki na temperaturę otoczenia.

**Słowa kluczowe:** analizy GIS, miejska wyspa ciepła, Landsat, temperatura radiacyjna, naturalny potencjał chłodzenia